

Global frequency of magnitude 9 earthquakes

Robert McCaffrey GNS Science, PO Box 30368, Lower Hutt, New Zealand

ABSTRACT

For decades seismologists have sought causal relationships between maximum earthquake sizes and other properties of subduction zones, with the underlying notion that some subduction zones may never produce a magnitude ~ 9 or larger event. The 2004 Andaman M_w 9.2 earthquake called into question such ideas. Given multicentury return times of the greatest earthquakes, ignorance of those return times and our very limited observation span, I suggest that we cannot yet make such determinations. Present evidence cannot rule out that any subduction zone may produce a magnitude 9 or larger earthquake. Based on theoretical recurrence times, I estimate that one to three M_9 earthquakes should occur globally per century, and the past half century with five M_9 events reflects temporal clustering and not the long-term average.

Keywords: subduction, earthquakes, earthquake recurrence, earthquake history.

INTRODUCTION

The world's truly great earthquakes, those of $M_w \geq 9$, occur very infrequently, but when they do the damage and loss of life can be enormous, as we witnessed in December 2004. Most great earthquakes occur at sub-

marine subduction zones where one tectonic plate slides at a gentle angle (10° – 30°) beneath another. They can rupture hundreds of kilometers of the fault and generate destructive tsunami waves that can have far-reaching effects (Titov et al., 2005). With more than

40,000 km of subduction boundaries (Fig. 1) and the rupture of any one contiguous segment of several hundred kilometers length sufficient to produce an $M_w \geq 9$, opportunities for them abound.

Seismologists have attempted to tie the history of earthquakes over the past century to various properties of subduction zones, such as convergence rate, slab age, fault temperature, and others, in order to understand what might limit earthquake size. In this paper I look at the probabilities of the largest earthquakes and, in the context of recurrence times and our short history of observation, argue that we cannot rule out an $M_w \geq 9$ earthquake at any subduction zone. Simulations using recurrence times of the maximum size earthquakes (called M_9) at subduction zones suggest that 1–3 M_9 earthquakes should occur within any 100 yr span.

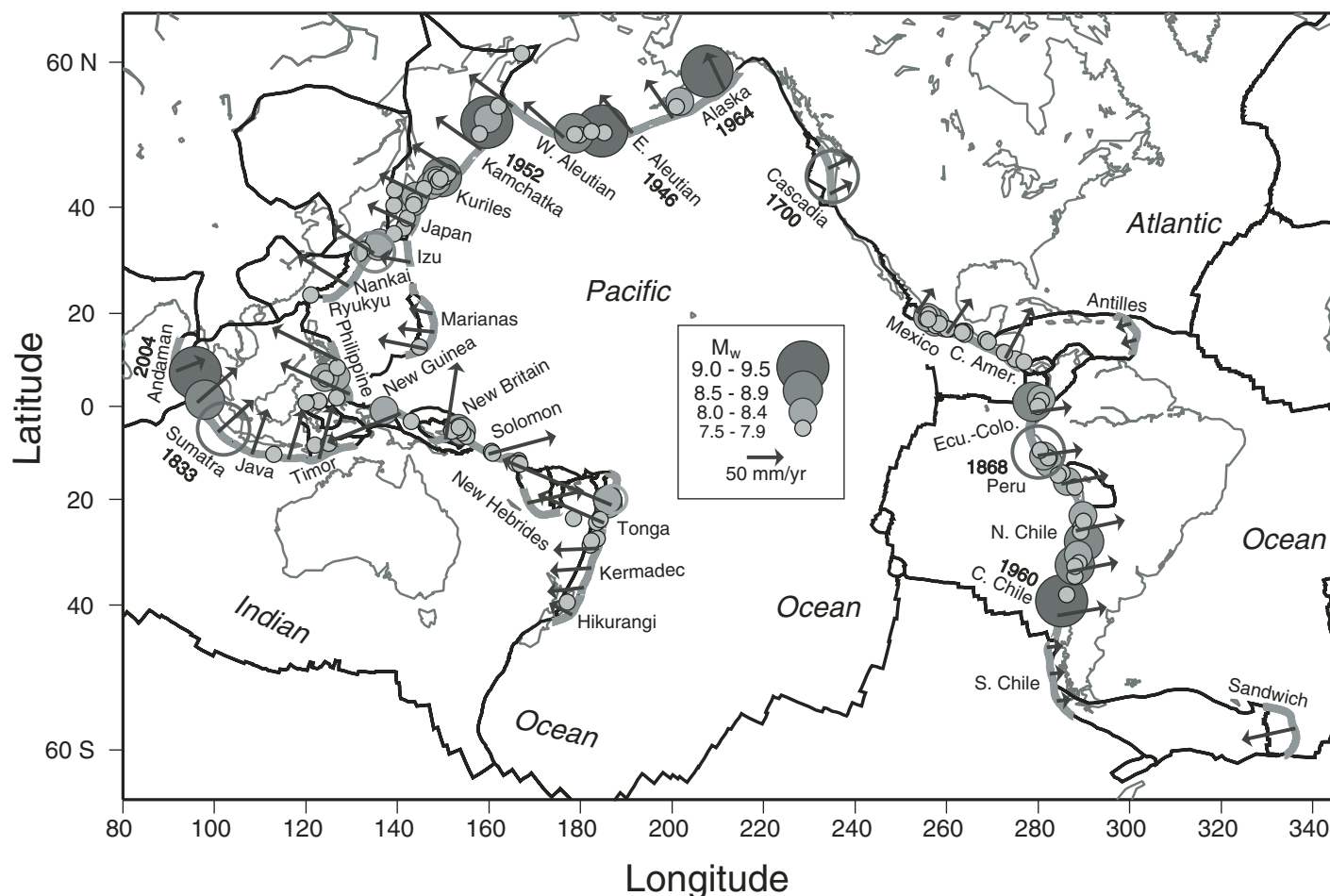


Figure 1. Map of world's major subduction zones (thick gray lines) and tectonic plate boundaries (Bird, 2003). Filled circles show locations of known earthquakes of $M_w \geq 7.5$ or greater since 1900 (circle radius and grayscaled by magnitude). Open circles are largest known earthquakes from A.D. 1700 to 1900 (compiled by Stein and Okal, 2007). Arrows show horizontal velocity of subducting plate relative to overriding plate. Dates are given for all M_9 quakes.

The five M9 events that have occurred since 1952 probably represent temporal clustering and not a long-term average.

EARTHQUAKE SIZE LIMITED BY SUBDUCTION ZONE PROPERTIES

It has been observed over the past century that some subduction zones produce larger earthquakes than others. Some, like Cascadia, Southern Chile, and the Marianas, appeared to be relatively aseismic. A question that arises is whether such century-scale differences represent an intrinsic, long-lived property of subduction zones. Early ideas held that if the subducting plate was young (hence, warm and buoyant) and coming in fast, its trajectory into the mantle would be shallow and it would stick more to the plate above it, leading to bigger quakes (Uyeda and Kanamori, 1979). The converse was that slow subduction of old lithosphere would produce only smaller quakes. A linear regression relating observed maximum earthquake magnitude to subducting plate age and convergence speed showed a significant correlation (Ruff and Kanamori, 1980). Later studies using improved data showed this correlation to be less compelling (Pacheco et al., 1993) or possibly related to nonmechanical factors (McCaffrey, 1997b). The 2004 Sumatra–Andaman Islands earthquake, which occurred in one of the “unlikely” subduction zones (i.e., where old lithosphere subducts slowly), clearly violated the Ruff and Kanamori (1980) relationship (Stein and Okal, 2007). Several other plausible mechanical explanations were suggested (Scholz and Campos, 1995; McCaffrey, 1993; Ruff, 1989; Ruff and Tichelaar, 1996), but all have significant exceptions when compared to the actual earthquake history.

High temperatures within the Earth promote ductile deformation, so that earthquakes may be smaller at subduction zones where young, hot lithosphere subducts slowly and warms up the fault zone (Tichelaar and Ruff, 1993). Regressions relating earthquake magnitudes to fault zone temperatures gave fits similar to those of the mechanical models (McCaffrey, 1997b). In both the mechanical and thermal processes, slow convergence tends to suppress great earthquake activity. Nevertheless, the Andaman subduction zone is among the world’s slowest (GSA Data Repository Table DR1¹), yet produced the third-largest earthquake documented. An alternative view is that because slow convergence also increases the recurrence time, in a finite time slow subduction zones are merely less likely to have a great earthquake.

¹GSA Data Repository item 2008063, Table DR1, data used in the study, is available online at www.geosociety.org/pubs/ft2008.htm, or on request from editing@geosociety.org or Documents Secretary, GSA, P.O. Box 9140, Boulder, CO 80301, USA.

RECURRENCE TIMES OF GREAT EARTHQUAKES

The questions are what governs the frequency of these massive earthquakes and whether or all subduction zones are capable of producing one. First, I define an M9 as the largest earthquake that can occur within a given segment of the plate boundary; i.e., one that ruptures the entire length of the segment (the segments, discussed in the following, are each long enough to produce an M9 earthquake). A first-order estimate of M9 earthquake recurrence can be gleaned from plate tectonics and a moment conservation principle (Kagan, 2002). If an M9 earthquake accounts for u meters of average slip on the boundary between the converging plates, then the long-term average time between them will be u/v , where v is the convergence rate (assuming all slip is by M9 quakes). Plate convergence rates vary from $v = 25$ mm/yr to 100 mm/yr, suggesting repeat times on the order of 250–1000 yr if $u = 25$ m, a reasonable amount for an M9 quake (Wells and Coppersmith, 1994). If some fraction of the convergence is taken up by other means such as creep, slow slip events, or smaller earthquakes, then this repeat time is increased accordingly, as discussed in the following.

From an observational point of view, this nominal multicentury time between M9 events is problematic because reliable records of earthquakes date back only a century in most places. Other information, such as written accounts and geologic observations, can be used to extend the history. In places where such data exist, the times between repeating great earthquakes are highly irregular. In Cascadia, for example, geologic observations related to earthquakes give an average time between events of 600 yr over the past 7700 yr (Goldfinger et al., 2003), yet the actual inter-event times range from ~215 to 1488 yr (assuming all events were identified), revealing a very large randomness to when the margin breaks.

Because we often glean the recurrence interval for great earthquakes from field observations of past events, I first examine how well the recurrence time can be estimated from such data. To do this, I use a Monte Carlo simulation, assuming a Poisson probability function (Feller, 1966). The probability of an M9 is $1/T$ during any given year, where T is the simulated M9 recurrence time in years. Figure 2 shows the recovery of T given an observed history of duration H . When $H \gg T$ (e.g., $H/T > 20$), T is fairly well estimated, but for $H/T < 10$ it is not. For Cascadia, for example, $H/T \sim 13$ ($H \sim 7700$ yr; $T \sim 600$ yr) and the standard deviation in T estimates will be ~200 yr ($T_\sigma \sim 0.3 T_{\text{actual}}$; Fig. 2) simply from a sampling perspective. For most other subduction zones, $H = 100$ yr and if $T \sim 500$ yr, then $H/T = 0.5$ and T will be unresolvable. Frohlich (2007) reaches similar conclusions regarding the completeness of earthquake catalogs.

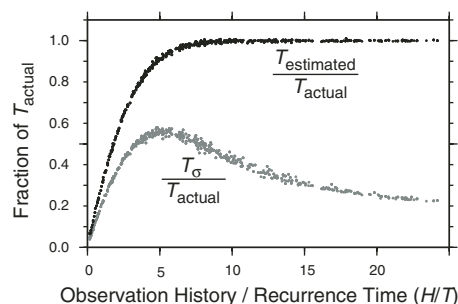


Figure 2. Simulations of recurrence time T estimates from 5000 Monte Carlo histories of observations of duration H . When $H/T < 5$, recurrence time is poorly estimated (low scatter in T_σ is due to small number of events when H/T is small). At high H/T , recurrence time is on average recovered but scatter in estimated T remains large. Obtaining T with high confidence (low T_σ) requires $H \gg T$.

EARTHQUAKE SIZE LIMITED BY SUBDUCTION ZONE LENGTH

Given that observation-based estimates of T from the short earthquake record are problematic, I make estimates based on theoretical considerations. For this purpose, the world’s subduction zones are divided into 32 segments based on changes in plate pairs converging, in rates or obliquity of convergence or natural geologic breaks (Fig. 1). Convergence rates for each segment are estimated using best available poles that take into account mobile forearcs (Table DR1; see footnote 1). The recurrence time of the segment-filling event, i.e., the largest possible earthquake on that segment, is calculated considering the length of the segment as the determining feature.

The seismic moment of the largest possible earthquake on a fault of length L is

$$M_o^{\text{max}} = \mu u_{\text{av}} L Z_{\text{max}} / \sin \delta, \quad (1)$$

where μ is the shear modulus, u_{av} is the average slip in the earthquake, Z_{max} is the maximum depth of slip (40 km used; Tichelaar and Ruff, 1993), and δ is the average fault dip angle (derived from earthquake mechanisms; Table DR1 [see footnote 1]). The recurrence time for this greatest earthquake is

$$T = u_{\text{av}} / f \chi v, \quad (2)$$

where v is the plate motion rate, f is the fraction of the total seismic moment in M9 earthquakes, and χ is the fraction of slip on the boundary that occurs seismically. Extrapolating the Wells and Coppersmith (1994) relationships between M and L and M and u suggests that $u_{\text{av}} \approx 2.5 \times 10^{-5} L$ (see also Liu-Zeng et al., 2005). Using Equations 1 and 2 to estimate M_w^{max} (where $M_w = 2/3 \log M_o - 6.07$, M_o in Nm) and T for each segment, each segment is capable of an M9 earthquake and globally the median

recurrence time for them is 490 yr (using $f = 1$, $\chi = 1$; Table DR1; see footnote 1).

The value of f , the ratio of the moment of the largest quake to the total seismic moment, can be gleaned from the β value derived from the cumulative frequency-magnitude relationship,

$$N(M_0) = \alpha M_0^{-\beta}, \quad (3)$$

where N is the number of earthquakes greater than or equal to M_0 , α and β are constants, and $f \approx 1 - \beta$ (see McCaffrey, 1997a, Fig. 1b; Feller, 1966). Kagan (1999) and Bird and Kagan (2004) estimated β for subduction zones to be in the range ~ 0.55 – 0.68 (Table DR1; see footnote 1); hence f is likely to be between 0.32 and 0.45. In some cases a constant β at large magnitudes underestimates the size of the largest earthquake, which then underestimates f . For this reason I run the simulations considering values for f other than those obtained from β .

In addition, aseismic slip takes up some of the convergence. The fraction χ , called the seismic coupling coefficient (Scholz, 1990), based on earthquake catalogs, is seen to vary greatly among subduction zones (Peterson and Seno, 1984; Pacheco et al., 1993; Scholz and Campos, 1995; Frohlich and Wetzell, 2007), but is very sensitive to the randomness of earthquake occurrence (McCaffrey, 1997a). We know from observed aseismic and postseismic slip and slow slip events that $\chi < 1$, but beyond that, long-term estimates are poor. Frohlich and Wetzell (2007) estimated a global value of 0.33, but individual values range from 0.07 to 0.7. In all calculations below I assume $\chi = 1$, which will minimize the recurrence times (maximizing M9 frequency). Accordingly, the recurrence time for an M9 could be 2 or more times longer than if all slip on the interface occurred by infrequent M9 earthquakes (i.e., when $f = 1$, $\chi = 1$).

Kagan (1999) showed that β values obtained from moderate sized earthquakes do not differ significantly among the subduction zones he studied, and suggested that it follows that there should not be a difference in the maximum earthquake magnitude at them. Inferences based on the incomplete 100 yr record of great earthquakes must be held suspect; there is no reason to expect that any of these margins cannot be the site of an M9.

COMPARING EXPECTED TO OBSERVED MAXIMUM M_w

The largest known earthquakes at subduction zones are compared to the largest expected according to Equation 1 plotted against their recurrence times (Fig. 3). Taking 0.4 magnitude units as the uncertainty level in M_w (combining errors in moment estimates and in my estimate of parameters that determine the largest events), it appears that five of the segments have possibly had their largest quakes during the past 100 yr

(Fig. 3). In fact, these five events occurred during A.D. 1952–2004 (Fig. 1).

Using the compilation of largest subduction zone earthquakes by Stein and Okal (2007) that goes back 300 yr, it appears that as many as eight segments may have had their maxima and others may be approaching it (keeping in mind that knowledge of earthquakes prior to 1900 is tenuous and some M9 events may have been missed). The average magnitude deficit (expected minus observed maximum M_w) for the past 100 yr is 1.4 magnitude units, while over the past 300 yr it decreases to 1.2. If the past 100 yr were representative of long-term earthquake behavior, these distributions would be the same.

As has been noted by many, and based on observational and theoretical arguments, the past 100 yr of earthquake history are not representative of longer term earthquake behavior on individual faults. Nevertheless, subduction seismicity models discussed earlier were validated by this incomplete earthquake record. For example, the largest known thrust earthquake at the Marianas subduction zone in the past 100 yr was only $M_w = 7.7$ (in 1983). Because of this, the Marianas is considered to represent the decoupled end-member subduction zone (Uyeda and Kanamori, 1979). However, the estimated M9 recurrence time for the Marianas is close to 900 yr and the probability of not having an M9 there during any 100 yr period is 89%.

M9 FREQUENCY SIMULATIONS

Given that we cannot rely on the incomplete record of the past to gain insight into long-term trends, I perform simulations of M9 occurrence without relying too strongly on the short earthquake history. Assuming that all 32 subduction segments are capable of producing an M9 and using the distribution of M9 recurrence times based on fault lengths and convergence rates

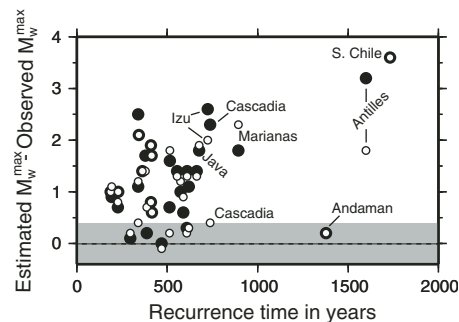


Figure 3. Plot of the difference between M_w of predicted largest earthquake and observed largest earthquake versus predicted recurrence time for such quakes at each subduction zone segment. Dots represent post-1900 quakes only, while open circles are post-1700 (from Stein and Okal, 2007). Gray area shows where M_w difference is < 0.4 magnitude units (error level in estimates).

(Equation 2), I estimate the probability that a number N of the largest possible quakes will occur at random within 100 yr. For this, I assume that the probability of the quake happening is $1/T$ for any one year, where T is the M9 recurrence time in years. T depends on the assumed value of f and so I use $f = 1$, $f = 2/3$, $f = 1/3$, and $f = 1 - \beta$ (using the β values estimated by Kagan [1999] for individual trenches).

The simulation is tied to historical earthquake data in two ways: (1) through the use of β , which is estimated from past seismicity, and (2) through the assumption that the average slip u_w scales with fault length L . Typically β is determined by fits to earthquake size distributions and is based on many events. The estimated values are close to the theoretical value of $2/3$ predicted by earthquake self-similarity arguments (Rundle, 1989). Because extrapolation of β to high magnitudes can sometimes underestimate the largest event, I also use larger f values that allow for more moment in the largest event. The slip/length ratio is estimated from many earthquakes and will probably not change much with additional data (Wells and Coppersmith, 1994). (For ranges of T based on ranges of v , β , and u_w , see footnote 1)

A Monte Carlo simulation is run for 30,000 centuries, and the probability distribution P of having N earthquakes in one century is calculated (Fig. 4). When more of the moment is in M9 quakes (higher f), the probability of having more M9 events increases (curves 1, 2,

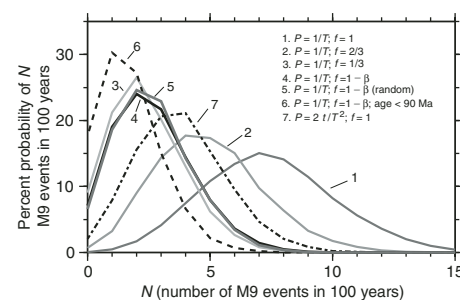


Figure 4. Histograms of the probability that number of (N) M9 earthquakes will occur randomly in any 100 yr period, given distribution of expected recurrence times at 32 subduction zone segments. Curves are labeled by values used in simulation (T is recurrence time; P = probability of an event during any year, f = fraction of moment that occurs in largest earthquake; value of χ , the fraction of total slip released by earthquakes, is 1.0 for all simulations). Simulations with “ $f = 1 - \beta$ ” use β values from individual subduction zones estimated by Kagan (1999) and simulation 5 randomly samples β values. Simulation 6 simulates subset of 22 subduction zones based on age younger than 90 Ma that can produce M9 earthquakes. All simulations except 7 use Poisson probability for M9 occurrence ($P = 1/T$); for simulation 7, P increases linearly with time t since last event.

and 3; Fig. 4). The number of M9 earthquakes that occurred in the past 100 yr (5) is most consistent with the expected number if I use only the predicted times where $f \approx 2/3$. If only $\sim 1/3$ of the slip is in M9s, consistent with observed β values, then the peak is lower, from 1 to 3 M9 events per century (curves 3–5; Fig. 4).

The recurrence-time concept is fundamentally different from the mechanical explanations in that the latter predict some subduction zones to be incapable of having an M9 while the former holds that they are merely improbable. In another Monte Carlo simulation, the probability of M9 was set to zero for 10 trench segments with subducting plate ages older than 90 Ma (curve 6; using $f = 1$). The distribution of M9 events looks similar to those where all trenches are capable of an M9 and $f = 1/3$. Finally, a test was conducted where the probability of an M9 increases linearly with time t after the previous event, $P(t) = 2t/T^2$. This simulation (curve 7; Fig. 4) revealed a much lower probability for events than curve 1, the $1/T$ trial with the same f value, because the probability of a second event following closely in time is greatly reduced in curve 7.

From the series of tests, I suggest that the expected rate of M9 earthquakes per century may be closer to 1–3 than to the 5 that occurred in the past 100 yr. If all M9 events over the past 300 yr have been included in the Stein and Okal (2007) compilation, then the number per century is close to 3 and the distribution using $f \approx 1/3$, in agreement with $\beta \approx 0.67$, is likely.

DISCUSSION AND CONCLUSIONS

The great earthquake in late 2004 surprised many scientists in that its main area of slip was to the northwest along the Andaman Islands, the unlikely quiet region, and not offshore Sumatra, an area with a rich earthquake history. The Andaman section of this plate boundary accommodates slow subduction of old lithosphere and is accompanied by backarc spreading; thus mechanically it was in the low-magnitude category. However, thermally it is very similar to the central Chile margin, where an M 9.5 earthquake occurred in 1960 (McCaffrey, 1997b). Clearly, our efforts to decipher the patterns of great earthquakes empirically have not been successful, most likely because we do not have a long enough record to observe the process. Past models of subduction zone seismicity have been based on a very incomplete record and thus cannot be validated by that record. It may be analogous to throwing 32 dice (possibly loaded?) one time and trying to glean the properties of the individual die that result in some of them coming up sixes and some not. Clearly several more throws will reveal whether or not that is a useful endeavor. For great earthquakes,

it may take many more centuries to understand a pattern, if one exists.

Due to the incomplete history of great subduction earthquakes, we cannot rule out any of these subduction zones as being capable of generating an M9 earthquake. Several are adjacent to densely populated islands, and the impacts of shaking and tsunami waves on them cannot be overstated. Java, in particular, has a predicted M9 recurrence time that is half that of the Andaman segment (Fig. 3) and is among the longest subduction segments (Table DR1; see footnote 1).

Simulations of the recurrences of M9 earthquakes based on the lengths of trenches and convergence rates suggest that the global occurrence of M9 earthquakes is 1–3 per century, and the 5 that occurred in the past 100 yr may be higher than long-term averages.

ACKNOWLEDGMENTS

Reviews by William Power, Stephen Bannister, Suzette Jackson Payne, and Yan Kagan improved the manuscript.

REFERENCES CITED

- Bird, P., 2003, An updated digital model of plate boundaries: *Geochemistry, Geophysics, Geosystems*, v. 4, p. 1027, doi: 10.1029/2001GC000252.
- Bird, P., and Kagan, Y.Y., 2004, Plate-tectonic analysis of shallow seismicity: Apparent boundary width, beta, corner magnitude, coupled lithosphere thickness, and coupling in seven tectonic settings: *Seismological Society of America Bulletin*, v. 94, p. 2380–2399, doi: 10.1785/0120030107.
- Feller, W., 1966, *An introduction to probability theory and its applications* (second edition): New York, Wiley, 626 p.
- Frohlich, C., 2007, Practical suggestions for assessing rates of seismic-moment release: *Seismological Society of America Bulletin*, v. 97, p. 1158–1166, doi: 10.1785/0120060193.
- Frohlich, C., and Wetzel, L.R., 2007, Comparison of seismic moment release rates along different types of plate boundaries: *Geophysical Journal International*, v. 171, p. 909–920, doi: 10.1111/j.1365-246X.2007.03550.x.
- Goldfinger, C., Nelson, C.H., Johnson, J.E., and the Shipboard Scientific Party, 2003, Holocene earthquake records from the Cascadia subduction zone and northern San Andreas fault based on precise dating of offshore turbidites: *Annual Review of Earth and Planetary Sciences*, v. 31, p. 555–577, doi: 10.1146/annurev.earth.31.100901.141246.
- Kagan, Y.Y., 1999, Universality of the seismic moment-frequency relation: *Pure and Applied Geophysics*, v. 155, p. 537–573, doi: 10.1007/s000240050277.
- Kagan, Y.Y., 2002, Seismic moment distribution revisited: II. Moment conservation principle: *Geophysical Journal International*, v. 149, p. 731–754.
- Liu-Zeng, J., Heaton, T., and DiCaprio, C., 2005, The effect of slip variability on earthquake slip-length scaling: *Geophysical Journal International*, v. 162, p. 841–849, doi: 10.1111/j.1365-246X.2005.02679.x.

- McCaffrey, R., 1993, On the role of the upper plate in great subduction zone earthquakes: *Journal of Geophysical Research*, v. 98, p. 11,953–11,966.
- McCaffrey, R., 1997a, Statistical significance of the seismic coupling coefficient: *Seismological Society of America Bulletin*, v. 87, p. 1069–1073.
- McCaffrey, R., 1997b, Influences of recurrence times and fault zone temperatures on the age-rate dependence of subduction zone seismicity: *Journal of Geophysical Research*, v. 102, p. 22,839–22,854, doi: 10.1029/97JB01827.
- Pacheco, J.F., Sykes, L.R., and Scholz, C.H., 1993, Nature of seismic coupling along simple plate boundaries of the subduction type: *Journal of Geophysical Research*, v. 98, p. 14,133–14,159.
- Peterson, E.T., and Seno, T., 1984, Factors affecting seismic moment release rates in subduction zones: *Journal of Geophysical Research*, v. 89, p. 10,233–10,248.
- Ruff, L.J., 1989, Do trench sediments affect great earthquake occurrence in subduction zones?: *Pure and Applied Geophysics*, v. 129, p. 263–282, doi: 10.1007/BF00874629.
- Ruff, L.J., and Kanamori, H., 1980, Seismicity and the subduction process: *Physics of the Earth and Planetary Interiors*, v. 23, p. 240–252, doi: 10.1016/0031-9201(80)90117-X.
- Ruff, L.J., and Tichelaar, B.W., 1996, What controls the seismogenic plate interface at subduction zones?, in Bebout, G.E., et al., eds., *Subduction: Top to bottom: American Geophysical Union Geophysical Monograph* 96, p. 105–111.
- Rundle, J., 1989, Derivation of the complete Gutenberg-Richter magnitude-frequency relation using the principle of scale invariance: *Journal of Geophysical Research*, v. 94, p. 12,337–12,342.
- Scholz, C.H., 1990, *The mechanics of earthquakes and faulting*: Cambridge, Cambridge University Press, 439 p.
- Scholz, C.H., and Campos, J., 1995, On the mechanism of seismic decoupling and backarc spreading at subduction zones: *Journal of Geophysical Research*, v. 100, p. 22,103–22,115, doi: 10.1029/95JB01869.
- Stein, S., and Okal, E.A., 2007, Ultralong period seismic study of the December 2004 Indian Ocean earthquake and implications for regional tectonics and the subduction process: *Seismological Society of America Bulletin*, v. 97, p. S279–S295, doi: 10.1785/0120050617.
- Tichelaar, B.W., and Ruff, L.J., 1993, Depth of seismic coupling along subduction zones: *Journal of Geophysical Research*, v. 98, p. 2017–2037.
- Titov, V., Rabinovich, A.B., Mofjeld, H.O., Thomson, R.E., and Gonzalez, F.I., 2005, The global reach of the 26 December 2004 Sumatra tsunami: *Science*, v. 309, p. 2045–2048, doi: 10.1126/science.1114576.
- Uyeda, S., and Kanamori, H., 1979, Back-arc opening and the mode of subduction: *Journal of Geophysical Research*, v. 84, p. 1049–1061.
- Wells, D.L., and Coppersmith, K.J., 1994, New empirical relationships among magnitude, rupture length, rupture width, rupture area and surface displacement: *Seismological Society of America Bulletin*, v. 84, p. 974–1002.

Manuscript received 11 September 2007

Revised manuscript received 19 November 2007

Manuscript accepted 29 November 2007

Printed in USA

Data Repository Item

“Global Frequency of Magnitude 9 Earthquakes” by R. McCaffrey

Table DR1 explanation.

Length – length of subduction thrust measured along strike.

Rate range - Range of convergence rates along subduction segment.

Rate source: Source of relative angular velocity between plates. a - Sella et al. (2002); b – Bird (2003); c – DeMets et al. (1994); d - McCaffrey et al. (2007); e – Wallace et al. (2005); f – Wallace et al. (2004a); g – Wallace et al. (2004b).

Dip – dip angle of thrust estimated from CMT solutions (McCaffrey, 1997).

Sip range – Range of expected slip during M9 earthquake. Derived using $u = 2.5 \pm 1.0 \times 10^{-5} L$ where L is length of thrust fault along strike.

β and σ – value of β from Kagan (1999), assumed values for Cascadia and Timor.

Predicted Mw max – predicted Mw of largest earthquake that can occur on the fault.

$$M_o^{max} = \mu u_{av} L Z_{max} / \sin \delta$$

$$M_w^{max} = 2/3 \log_{10} (M_o^{max} - 9.1)$$

Maximum fault depth $Z_{max} = 40$ km (Tichelaar and Ruff, 1993), fault length L and fault dip δ taken from individual faults, $\mu = 30$ GPa. $u_{av} = 2.5 \times 10^{-5} L$.

Obs. Mw max, 100 year – observed largest thrust earthquake at trench during last 100 years. (Kanamori, 1983; Engdahl and Villasenor, 2002; Harvard CMT).

Obs. Mw max, 300 year – observed largest thrust earthquake at trench during last 300 years, taken from Stein and Okal,(2007).

Recurrence time – Nominal time between M9 earthquakes using

$$T = u_{av} / f \chi v$$

where $u_{av} = 2.5 \times 10^{-5} L$, v is the convergence rate, $f = 1$, and $\chi = 1$.

Recurrence time range – Range of times between M9 earthquakes estimated from ranges of v , β and u_{av} , where $f = 1 - \beta$.

Age – age of the subducting plate in Millions of years (McCaffrey, 1997).

Plate pairs (HW = hanging wall; FW = footwall)– plates meeting at subduction zones.

Abbreviations: An – Antarctic; Au – Australia; Bu – Burma; Ca – Caribbean; Co – Cocos; Cs – South China; Hf – Hikurangi forearc; In – Indian; Jf – Juan de Fuca; Ma – Marianas forearc; Na – North America; Nz – Nazca; Ok – Okhtosk; Or – Oregon forearc; Pa – Pacific; Ph – Philippine; Sa – South America; Sf – Sumatra forearc; Su – Sunda; Sw – Sandwich; To – Tonga forearc.

Citations

- Bird, P. (2003). An updated digital model of plate boundaries, *Geochem. Geophys. Geosystems* 4, 1027, doi 10.1029/2001GC000252.
- DeMets, C., R. G. Gordon, D. F. Argus, and S. Stein (1994). Effects of recent revisions to the geomagnetic reversal time scale on estimates of current plate motions, *Geophys. Res. Letters* 21, 2191-2194.
- Engdahl, E.R. and A. Villasenor (2002). Global seismicity: 1900-1999, in *IASPEI Handbook of Earthquake and Engineering Seismology* (W. H. K. Lee, H. Kanamori, P. C. Jennings, and C. Kisslinger, Editors), pp. 665-690, Boston, Academic Press.
- Kagan, Y. Y. (1999). Universality of the seismic moment-frequency relation, *Pure Appl. Geophys.* 155, 537–573.
- Kanamori, H., (1983). Global Seismicity, in *Earthquakes: Observation, theory and interpretation*, edited by H. Kanamori and E. Bosch, pp. 597, North Holland, New York.
- McCaffrey, R., (1997). Influences of recurrence times and fault zone temperatures on the age-rate dependence of subduction zone seismicity, *Journal of Geophysical Research*, 102, 22,839-22,854.
- McCaffrey, R., A. I. Qamar, R. W. King, R. Wells, Z. Ning, C. A. Williams, C. W. Stevens, J. J. Vollick, and P. C. Zwick, (2007). Plate locking, block rotation and crustal deformation in the Pacific Northwest, *Geophys. J. Int.*, doi:10.1111/j.1365-246X.2007.03371.x.
- Sella, G. F., T. H. Dixon, and A. Mao (2002), REVEL: A model for recent plate velocities from space geodesy, *J. Geophys. Res.*, 107, doi:10.1029/2000JB000033.
- Stein, S. and E. A. Okal (2007). Ultralong period seismic study of the December 2004 Indian Ocean earthquake and implications for regional tectonics and the subduction process, *Bull. Seism. Soc. Am.* 97, S279-S295, doi: 10.1785/0120050617.
- Tichelaar, B. W., and L. J. Ruff, (1993). Depth of seismic coupling along subduction zones, *J. Geophys. Res.*, 98, 2017-2037.
- Wallace, L.M., C. W. Stevens, E. Silver, R. McCaffrey, W. Loratung, S. Hasiata, R. Curley, R. Rosa, J. Taugaloidi, and H. Davies, (2004a). GPS Constraints on Active Tectonics and Arc-Continent Collision in Papua New Guinea: evidence for edge-driven microplate rotations, *J. Geophys. Res.*, 109, doi:10.1029/2003JB002481.

- Wallace, L. M., J. Beavan, R. McCaffrey, and D. Darby (2004b), Subduction zone coupling and tectonic block rotations in the North Island, New Zealand, *J. Geophys. Res.*, 109, B12406, doi:10.1029/2004JB003241.
- Wallace, L. M., R. McCaffrey, J. Beavan, and S. Ellis (2005), Rapid microplate rotations and back-arc rifting at the transition between collision and subduction, *Geology*, 33, 857-860.

Table DRI.

No.	Trench Name	Length, km	Rate range, mm/yr	Rate source	Dip, °	Dip sigma, °	Slip range, meters	β	β sigma	Predicted max Mw	Obs. Max Mw 100 yr	Obs. Max Mw 300 yr	Recurrence Time, years	Recurr. Time range, years	Age, Ma	Plate HW	Pairs FW
1	ALASKA	1489	55-66	a	18	7	22-52	0.59	0.05	9.5	9.2	9.3	606	872-2146	49	Na	Pa
2	ANDAMAN	1701	16-44	b	24	3	25-59	0.72	0.13	9.5	9.3	9.3	1379	2091-8739	83	Bu	In
3	ANTILLES	1228	17-21	a	25	9	18-43	0.59	0.11	9.3	6.1	7.5	1600	2066-6381	87	Ca	Na
4	C. AMERICA	1506	62-83	c	22	6	22-52	0.68	0.07	9.4	7.8	7.6	513	894-2473	16	Ca	Co
5	C. CHILE	1304	63-75	a	13	6	19-45	0.56	0.05	9.5	9.5	9.6	468	620-1534	23	Sa	Nz
6	CASCADIA	1048	32-38	d	9	3	15-36	0.50	0.20	9.5	7.2	9.1	737	614-2861	5	Or	Jf
7	E. ALEUTIAN	1092	64-76	a	21	6	16-38	0.59	0.05	9.3	9.1	8.6	385	552-1363	56	Na	Pa
8	ECU-COLOM	1358	52-63	a	22	5	20-47	0.56	0.05	9.4	8.8	8.5	588	777-1922	21	Sa	Nz
9	HIKURANGI	781	22-48	g	20	10	11-27	0.79	0.04	9.1	7.7	7.8	553	1385-3865	100	Hf	Pa
10	IZU	1167	34-46	e	26	6	17-40	0.81	0.11	9.2	6.6	7.2	723	1739-4619	145	Ph	Pa
11	JAPAN	654	62-81	a	22	7	9-22	0.57	0.04	9.0	8.3	8.2	226	311-762	132	Ok	Pa
12	JAVA	1849	61-74	a	20	11	27-64	0.67	0.06	9.6	7.8	7.7	675	1171-3069	75	Su	Au
13	KAMCHATKA	907	69-84	a	30	6	13-31	0.57	0.04	9.1	9.0	8.9	294	399-977	115	Ok	Pa
14	KERMADEC	1421	50-66	a	24	7	21-49	0.79	0.04	9.4	8.0	8.1	609	1605-3966	100	Au	Pa
15	KURILES	1242	69-82	a	26	8	18-43	0.57	0.04	9.3	8.5	8.5	410	561-1371	128	Ok	Pa
16	MARIANAS	1812	31-70	e	25	8	27-63	0.81	0.11	9.5	7.7	7.2	893	1990-6165	134	Ma	Pa
17	MEXICO	1378	42-61	b	21	7	20-48	0.58	0.06	9.4	8.0	8.1	663	900-2344	9	Na	Co
18	N. CHILE	1581	63-74	a	22	8	23-55	0.56	0.05	9.5	8.5	8.3	573	762-1887	41	Sa	Nz
19	NANKAI	923	59-76	a	21	7	13-32	0.66	0.10	9.2	8.1	8.8	339	528-1607	23	Cs	Ph
20	NEW BRITAIN	867	75-157	f	20	3	13-30	0.61	0.04	9.1	8.1	8.1	186	268-728	50	Sb	Wk
21	NEW GUINEA	1030	103-121	a	20	10	15-36	0.57	0.05	9.2	8.2	8.2	229	312-768	100	Au	Pa
22	NEW HEBRIDES	1187	70-86	a	28	8	17-41	0.60	0.04	9.2	7.5	7.8	378	561-1364	40	Pa	Au
23	PERU	1599	58-70	a	22	8	23-55	0.56	0.05	9.5	8.4	9.2	618	806-2020	37	Sa	Nz
24	PHILIPPINE	1512	95-113	a	25	9	22-52	0.61	0.05	9.4	8.0	8.0	361	539-1355	43	Su	Ph
25	RYUKYU	1131	74-92	a	25	8	16-39	0.66	0.10	9.2	6.7	8.0	339	525-1619	46	Cs	Ph
26	S. CHILE	1218	15-19	a	25	3	18-42	0.56	0.05	9.3	5.7	5.7	1734	2304-5731	16	Sa	An
27	SANDWICH	1000	63-82	b	27	7	15-35	0.67	0.06	9.1	7.0	7.0	343	579-1573	57	Sw	Sa
28	SOLOMON	1585	86-105	a	20	3	23-55	0.61	0.04	9.5	7.8	7.8	412	626-1522	50	Pa	Au
29	SUMATRA	1393	60-75	b	20	9	20-48	0.72	0.13	9.4	8.7	9.2	512	925-2862	61	Sf	Au
30	TIMOR	1256	69-84	a	20	10	18-43	0.67	0.06	9.4	7.5	7.5	409	709-1864	100	Su	Au
31	TONGA	1450	125-252	e	24	7	21-50	0.79	0.04	9.4	8.5	8.3	191	479-1321	100	To	Pa
32	W. ALEUTIAN	1244	69-80	a	22	8	18-43	0.59	0.05	9.3	8.7	8.7	414	593-1471	72	Na	Pa